Viscosity of Dilute Model Bead Arrays at Low Shear: Inclusion of Short Range Solute−Solvent Interactions

Stuart A. Allison,* Hongxia Pei, Saerom Baek, Jennifer N. Garcia, Min Y. Lee, Vu Nguyen, and Umar T. Twahir

Department of Chemistry, Georgia State University, Atlanta, Georgia 30302-4098

Received: July 23, 2009; Revised Manuscript Received: August 18, 2009

The intrinsic viscosity, $[\eta]$, of certain polymer−solvent systems, such as alkanes in benzene, are "anomalous" in the sense that $[\eta]$ for low molecular weight fractions are low and in certain cases negative (Dewan, K. K.; Bloomfield, V. A.; Berget, P. G.; *J. Phys. Chem.* **1974**, *75*, 3120). In this work, the theory of the viscosity of a dilute suspension of macromolecules at low shear is formulated that accounts for possible solute−solvent interactions. In doing so, we show that negative intrinsic viscosities are possible and are able to reproduce quite well the known length dependence of $[\eta]$ for alkanes in benzene. The coarse grained, solvent continuum, bead model developed here is an extension of previous work (Allison, S. A.; Pei, H. *J. Phys. Chem. B* **2009**, *113*, 8056). Following Fixman (Fixman, M. *J. Chem. Phys.* **1990**, *92*, 6858), we assume that solute−solvent interactions are short-range in character and can be separated from long-range hydrodynamic interactions between different beads. These interactions are accounted for by introducing three adjustable parameters specific to the transport of small "monomeric" solutes in the solvent of interest. Long range hydrodynamic interactions are accounted for to order a_J^2/r_{IJ}^3 (a_J is a bead radius and r_{IJ} is an interbead distance). In modeling a macromolecule as an arbitrary array of N beads, the transport of the array is examined numerically in 5 different elementary shear fields. The most computationally demanding component of the procedure involves the inversion of a $12N$ by $12N$ matrix. In the present work, we restrict ourselves to systems with a maximum N of about 100. Our procedure is first applied to short rods and rings of from 2 to 10 beads which can be compared with independent results from the literature. Agreement is found to be better than 5%. Modeling macromolecules as wormlike chains, the procedure is then applied first to duplex DNA and then to alkanes in benzene. In both cases, it is possible to obtain excellent agreement between modeling and experiment.

I. Introduction

Modeling the intrinsic viscosity of general solutes present in dilute solution remains a challenging problem to this day. Much of this modeling is based on the "standard" model (S model for brevity) which works well when the solute is large in size relative to the solvent molecules in which it is immersed and solute/solvent interactions can be ignored, to a good approximation, beyond contact interactions at the solute−solvent interface. This model always predicts a positive intrinsic viscosity, which is at variance with experiment for certain systems such as low molecular weight alkanes in benzene[1] as well as other low molecular weight polymers in certain solvents.[2] Although amino acids and short peptides in aqueous solvent have positive intrinsic viscosities,[3] the S model is unable to account quantitatively for the experimental results.[4] One objective of the present work is to generalize the S model in a preliminary attempt to deal with this problem.

In the S model, the solute is represented as a rigid, possibly irregularly shaped particle, or rigid bead array, immersed in a continuum incompressible Newtonian fluid (the solvent) of viscosity η_0. Solute−solvent interactions are assumed to arise strictly from short-range excluded volume repulsions present at the solute−solvent interface. It is also assumed that the solvent obeys the low Reynolds Number Navier−Stokes equation (5, 6). In most applications of the S model, solute and solvent velocities are assumed to match at their interface ("stick" hydrodynamic boundary conditions). In the case of "slip" boundary conditions, only the velocity components normal to the interface match and the hydrodynamic stress forces at the interface are also assumed to be normal.[7] The applications of the S model discussed in the present work employ "stick" boundary conditions.

Using the S model, Einstein determined the intrinsic viscosity of dilute suspensions of spheres.[8] Extension of the model to axially symmetric ellipsoids proved problematic. Jeffrey correctly evaluated the energy dissipation of an ellipsoid in an arbitrary shear field,[9] but he did not carry out a suitable ensemble average to relate this to intrinsic viscosity. This was achieved by Simha in the limit of low shear[10] and by Scheraga under general shear conditions.[11] A key feature of the Simha−Scheraga treatment involved accounting for rotational Brownian motion. Ignoring Brownian motion leads to an underestimation of the intrinsic viscosity.[11] The S model (with account of Brownian motion) was extended to flexible polymers modeled as strings of beads by Kirkwood and co-workers.[12] This "bead method" has been refined and generalized (retaining the S model assumptions) by later investigators and applied to particles of arbitrary shape.[14−18] These latter applications, in which the surface of an irregularly shaped particle is modeled as a shell of closely packed beads, is similar to boundary element procedures, where it is modeled as a closed surface of interconnected triangular plates.[19,20] Current applications[18,20] can handle several thousand beads or plates and the boundary

* To whom correspondence should be addressed. E-mail: sallison@gsu.edu.

10.1021/jp907020j CCC: $40.75
Published on Web 09/22/2009

element procedure can accommodate "stick" or "slip" hydrodynamic boundary conditions.[19]

As discussed previously, one objective of the present work is to generalize the S model to account more accurately for solute−solvent interactions. This shall be done in a way that preserves many of the features of the "bead method".[13−18] The approach we shall follow is very similar to that of Fixman.[21] General, but *short-range* solute−solvent interactions are accounted for using single bead translational friction, rotational friction, and viscosity shape factors for individual beads that may be different from those of beads that interact with the solvent under standard (S model) conditions. *Long range* hydrodynamic interactions are treated in the same way as before.

A second objective of the present work involves taking approximate account of the variation in hydrodynamic stresses over individual beads. The present work is an extension and improvement upon our earlier treatment of this problem.[4] Accounting for this variation results in a significant improvement in accuracy when the model consists of a limited number of beads. In modeling, this makes it possible to sample many conformations of large extended structures, such as wormlike chains of duplex DNA consisting of 100 to over 600 base pairs in length, at low computational cost.

In section II, the methodology used to generalize the S model applied to structures represented by bead arrays is developed. In section III, this methodology is first applied to linear strings and rings of touching beads in order to test its accuracy. Later, it is applied first to duplex DNA in aqueous media, and then to alkanes in benzene. The latter system is one which cannot be explained well by the S model, but the generalization developed in this work is shown to account quite well for the intrinsic viscosities observed experimentally.

It is appropriate to discuss the limitations of the present approach at this stage. First, since the solvent is modeled as a continuum, the methodology developed here is coarse grained and strictly limited to distance scales that are comparable to or greater than the size of the solvent molecules themselves. For this reason or else for reasons of computational efficiency, the fundamental bead unit typically represents a grouping of many atoms. A second limitation concerns hydrodynamic boundary conditions. Although stick boundary conditions are appropriate under most conditions, slip boundary conditions are more appropriate for small molecules in nonpolar solvents.[22] Boundary element methodologies have been developed that are appropriate for these systems.[7,19] For the comparatively large systems of interest in the present work, the coarse graininess of our modeling makes strict adherence to (atomic scale) solute−solvent boundary conditions of lesser importance than for small solute particles. Since stick boundary conditions are more easily implemented, they are used throughout the present work. A third limitation arises from our assumption that direct forces are short-range in nature. Because of this assumption, the present approach cannot be applied to the primary electroviscous effect, which is particularly important for highly charged macroions at low salt.[23−25]

II. Theory/Methodology

II.A. Model. The solute is represented as an N bead array and is depicted in Figure 1. Bead J ($1 \le J \le N$) consists of an inner solid core of radius a_J and an outer fluid surface of radius b_J. In general, these radii can vary from bead to bead. The outer bead radii do not overlap. Stick hydrodynamic boundary conditions are assumed to prevail on the inner core bead surfaces, but an external force/volume, $\mathbf{s}(\mathbf{x})$, may be present in the fluid domain exterior to a_J, but interior to b_J, V_{eJ}. In the present work, it is useful to view $\mathbf{s}(\mathbf{x})$ as arising from the short-range solute−solvent interactions that may represent "solvent breaking" or "solvent stabilizing" influences that arise when the solute is placed in the solvent. In the present work, it shall be assumed that the solute is present in dilute concentration and that solute−solute interactions (interactions between different bead arrays) can be neglected. Outside of the V_{eJ}'s, it is assumed that $\mathbf{s}(\mathbf{x})$ can be set zero. The bead array is immersed in a simple shear field with shear gradient γ (in $\sec^{-1}$), and it is assumed that $1/\gamma$ is long on the time scale of the array's Brownian translational and rotational motions. It is also assumed that γ is sufficiently small so that deformation of the bead array can be ignored and that its average orientation remains isotropic. Let the bead array translate with instantaneous overall velocity, $\mathbf{u}_0$, relative to a center of rotation, $\mathbf{d}$. Also let the instantaneous angular velocity of the entire bead array about $\mathbf{d}$ be denoted by $\boldsymbol{\omega}$, and let $\mathbf{x}_K$ denote the instantaneous position of the center of bead K. By "instantaneous", we mean a time scale short compared to average translational and rotational displacements of the beads, but long compared to the impulsive collision time between beads and solvent. If point $\mathbf{y}$ lies on the fluid/inner core surface of bead K and stick boundary conditions hold, then the rigid body particle velocity and fluid velocities match at $\mathbf{y}$.

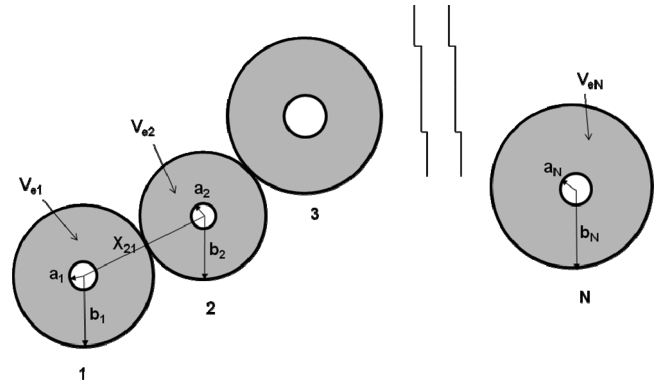

Figure 1. Schematic of the bead array model. Inner bead radii are denoted by a_I and external forces may be present out to a distance b_I from the center of bead I. These radii may vary from bead to bead. V_{eI} denotes the fluid volume between a_I and b_I. There are a total of N beads in the array and x_{IJ} denotes the distance between the centers of beads I and J.

$$\mathbf{v}_{\mathrm{RBM}}(\mathbf{y}) = \mathbf{u}_0 + \omega\, x\, (\mathbf{x}_K - \mathbf{d}) + \omega\, x\, (\mathbf{y} - \mathbf{x}_K) \quad (1)$$

In eq 1 above, "x" denotes the vector cross product.

Suppose our bead array is placed in a simple shear field where at $\mathbf{y}$, the fluid velocity in the absence of our bead array is given by

$$\mathbf{v}_0(\mathbf{y}) = \gamma \mathbf{e}_A(\mathbf{e}_B \cdot \mathbf{y}) \quad (2)$$

where $\mathbf{e}_A$ and $\mathbf{e}_B$ are arbitrary, but orthogonal unit vectors ($\mathbf{e}_A \cdot \mathbf{e}_B = 0$). It is convenient to break up eq 2 into pure translational, rotational, and deformational flows,

$$\mathbf{v}_0(\mathbf{y}) = \gamma(\mathbf{d} \cdot \mathbf{e}_B)\mathbf{e}_A + \frac{1}{2}\gamma(\mathbf{y} - \mathbf{d})\, x\, \mathbf{e}_C + \frac{1}{2}\boldsymbol{E} \cdot (\mathbf{y} - \mathbf{d}) \quad (3)$$

$$\mathbf{e}_C = \mathbf{e}_A x \mathbf{e}_B \tag{4}$$

$$\boldsymbol{E} = \gamma(\boldsymbol{e}_A\boldsymbol{e}_B + \boldsymbol{e}_B\boldsymbol{e}_A) \tag{5}$$

The second term on the right-hand side of eq 3 represents rotational motion of the fluid in the absence of the bead array about position **d**. We denote this angular velocity $\boldsymbol{\omega}_0$ and

$$\boldsymbol{\omega}_0 = -\frac{\gamma}{2}\mathbf{e}_C \tag{6}$$

When our bead array is placed in a flow field described by eq 2, it will translate with velocity $\mathbf{u}_0 = \gamma\,(\mathbf{d}\cdot\mathbf{e}_B)\mathbf{e}_A$. In the limit of negligible Brownian motion, it will also rotate, but its instantaneous angular velocity, $\boldsymbol{\omega}$, may be different from $\boldsymbol{\omega}_0$. For the cases of greatest interest in this work, Brownian motion is not negligible and indeed is quite significant. For the moment, however, it shall be left unaccounted for until the methodology is developed further. Under these conditions then, the total instantaneous force and torque exerted by the bead array on the fluid vanishes. We shall return to this point later. The first two terms in eq 3 represent the local translational and rotational motions of the fluid and the final term represents the deformational motion. This last term is particularly important in determining how the bead array affects the overall viscosity of the fluid.

Exterior to the inner core of the bead surfaces, the fluid is assumed to obey the low Reynolds number Navier−Stokes and solvent incompressibility equations (5, 6)

$$\eta_0\nabla^2\mathbf{v}(\mathbf{x}) - \nabla p(\mathbf{x}) = -\mathbf{s}(\mathbf{x}) \tag{7}$$

$$\nabla\cdot\mathbf{v}(\mathbf{x}) = 0 \tag{8}$$

where η_0 is the solvent viscosity, $\mathbf{v}(\mathbf{x})$ is the local fluid velocity at point **x** in the fluid, $p(\mathbf{x})$ is the local pressure, and $\mathbf{s}(\mathbf{x})$ is the local external force/unit volume discussed previously. The hydrodynamic stress tensor at any point in the fluid is given by[5,6]

$$\sigma(\mathbf{x}) = -p(\mathbf{x})\boldsymbol{I} + \eta_0(\nabla\boldsymbol{v}(\mathbf{x}) + \nabla\boldsymbol{v}(\mathbf{x})^{\mathrm{T}}) \tag{9}$$

where **I** is the 3 by 3 identity tensor and the "T" superscript denotes transpose. Before proceeding with the model development, it will be helpful to review the viscosity theory of a Newtonian fluid containing dilute solute particles represented as irregularly shaped (rigid) objects.

II.B. Viscosity of a Dilute Suspension of Irregularly Shaped Rigid Particles. The viscosity of a Newtonian fluid in the absence of solute, η_0, subjected to a simple shear field defined by eq 2 is related to $\boldsymbol{\sigma}_0$ (hydrodynamic stress in the absence of solute) by

$$\eta_0\gamma = \mathbf{e}_A\cdot\sigma_0(\mathbf{x})\cdot\mathbf{e}_B \tag{10}$$

This is readily verified by substituting eq 3 into eq 9 on the right-hand side of eq 10. The presence of dilute solute of number concentration c (in particles/dm^3) alters the long-range flow pattern (p, **v**, and $\boldsymbol{\sigma}$) in the fluid and this, in turn, alters the macroscopic viscosity, η, of the solution

$$\eta\gamma = \mathbf{e}_A\cdot\sigma(\mathbf{x})\cdot\mathbf{e}_B \tag{11}$$

The macroscopic excess stress, $\boldsymbol{\sigma}^e = \boldsymbol{\sigma} - \boldsymbol{\sigma}_0$, can be expressed in terms of single particle averages using an equation derived by Batchelor[26] (for fluids with $\mathbf{s}(\mathbf{x}) = 0$) and extended by Russell[27] to include external forces

$$\frac{\sigma^{\mathrm{e}}}{c} = -\Big\langle \int_{S_{\mathrm{p}}} \{\mathbf{f}(\mathbf{x})\mathbf{x} + \eta_0[\mathbf{v}(\mathbf{x})\,\mathbf{n}(\mathbf{x}) + \mathbf{n}(\mathbf{x})\,\mathbf{v}(\mathbf{x})]\}\,\mathrm{d}S_x + \int_{V_{\mathrm{e}}} \mathbf{s}(\mathbf{x})\,\mathbf{x}\,\mathrm{d}V_x\Big\rangle \tag{12}$$

In eq 12, brackets $\langle\ \rangle$ denote averaging over all possible particle positions and orientations, the surface integration over S_{p} is over the surface of the particle, which in the present case is the inner core surfaces of all N beads, $\mathbf{n}(\mathbf{x})$ denotes the local outward unit surface normal (into the fluid), the volume integral is over the fluid external to our particle, and

$$\mathbf{f}(\mathbf{x}) = -\sigma(\mathbf{x})\cdot\mathbf{n}(\mathbf{x}) \tag{13}$$

denotes the local hydrodynamic force/area exerted by the particle on the fluid. For a particle with stick hydrodynamic boundary conditions, both terms containing **v** on the right-hand side of eq 12 vanish. For our bead array model, the $i-j$ component of eq 12 can be written

$$\frac{\sigma_{ij}^{e}}{c} = -\sum_{K=1}^{N}\Big\langle \int_{S_K} f_i(\mathbf{x})\,x_j\,\mathrm{d}S_x + \int_{V_{eK}} s_i(\mathbf{x})\,x_j\,\mathrm{d}V_x\Big\rangle \tag{14}$$

It is useful to define a dimensionless "shape factor", ξ, by the relation

$$\xi = \lim_{c\to 0}\frac{1}{cV_{\mathrm{p}}}\left(\frac{\eta}{\eta_0} - 1\right) \tag{15}$$

$$V_{\mathrm{p}} = \sum_{K=1}^{N} V_K = \frac{4\pi}{3}\sum_{K=1}^{N} a_K{}^3 \tag{16}$$

For the special case of a spherical particle with $\mathbf{s}(\mathbf{x}) = 0$, $\xi = {}^5/_2$ as derived by Einstein.[8] The shape factor is closely related to the viscosity "B-factor", in dm^3/mol,

$$B = \lim_{c\to 0}\frac{N_{\mathrm{Av}}}{c}\left(\frac{\eta}{\eta_0} - 1\right) \tag{17}$$

and intrinsic viscosity, $[\eta]$, in dm^3/g

$$[\eta] = \lim_{c'\to 0}\frac{1}{c'}\left(\frac{\eta}{\eta_0} - 1\right) \tag{18}$$

where N_{Av} is Avogadro's Number and c' is the weight concentration of solute in g/dm^3. Let M denote the solute molecular weight, in g/mol, then ξ, B, and $[\eta]$ are related to each other by

$$B = N_{\mathrm{Av}} V_{\mathrm{P}} \xi = M[\eta] \tag{19}$$

Using eqs 10, 11, and 14 in eq 15

$$\xi = -\frac{1}{\eta_0 \gamma V_{\mathrm{P}}} \sum_{K=1}^{N} \mathbf{e}_A \cdot \langle \int_{S_K} \mathbf{f}(\mathbf{x})(\mathbf{x} - \mathbf{d})\, \mathrm{d}S_x + \int_{V_{eK}} \mathbf{s}(\mathbf{x})(\mathbf{x} - \mathbf{d})\, \mathrm{d}V_x \rangle \cdot \mathbf{e}_B \tag{20}$$

The inclusion of $\mathbf{d}$ in eq 20, or any other constant vector for that matter, is allowed because the total force, $\mathbf{F}_{\mathrm{total}}$, exerted by the bead array on the fluid vanishes for all conformations and/or orientations,

$$\mathbf{F}_{\mathrm{total}} = \sum_{K=1}^{N} \{ \int_{S_K} \mathbf{f}(\mathbf{x})\, \mathrm{d}S_x + \int_{V_{eK}} \mathbf{s}(\mathbf{x})\, \mathrm{d}V_x \} = 0 \tag{21}$$

To carry out the averages indicated in eq 20 for an arbitrary conformation of our bead array, it is necessary to examine the bead array in five different elementary shear fields,[19,25] which can be written

$$\boldsymbol{E}^{(1)} = \gamma(\boldsymbol{e}_1\boldsymbol{e}_2 + \boldsymbol{e}_2\boldsymbol{e}_1) \tag{22a}$$

$$\boldsymbol{E}^{(2)} = \gamma(\boldsymbol{e}_3\boldsymbol{e}_1 + \boldsymbol{e}_3\boldsymbol{e}_1) \tag{22b}$$

$$\boldsymbol{E}^{(3)} = \gamma(\boldsymbol{e}_2\boldsymbol{e}_3 + \boldsymbol{e}_3\boldsymbol{e}_2) \tag{22c}$$

$$\boldsymbol{E}^{(4)} = \gamma(\boldsymbol{e}_1\boldsymbol{e}_1 - \boldsymbol{e}_2\boldsymbol{e}_2) \tag{22d}$$

$$\boldsymbol{E}^{(5)} = \gamma(\boldsymbol{e}_1\boldsymbol{e}_1 - \boldsymbol{e}_3\boldsymbol{e}_3) \tag{22e}$$

In eqs 22, $\mathbf{e}_1$, $\mathbf{e}_2$, and $\mathbf{e}_3$ are orthogonal unit vectors in some convenient laboratory frame. Choosing $\mathbf{e}_A = \mathbf{e}_1$, $\mathbf{e}_B = \mathbf{e}_2$, then orientational averaging, assuming an isotropic distribution, yields[19,25]

$$\xi = \frac{1}{5}(\xi_{12}^{(1)} + \xi_{13}^{(2)} + \xi_{23}^{(3)}) + \frac{1}{15}(\xi_{11}^{(4)} + \xi_{33}^{(4)} - 2\xi_{22}^{(4)} + \xi_{11}^{(5)} + \xi_{22}^{(5)} - 2\xi_{33}^{(5)}) \tag{23}$$

where

$$\xi_{ij}^{(t)} = -\frac{1}{2\eta_0 \gamma V_{\mathrm{p}}} \sum_{K=1}^{N} \{ \int_{S_K} \mathbf{p} \cdot (\boldsymbol{e}_i\boldsymbol{e}_j + \boldsymbol{e}_j\boldsymbol{e}_i) \cdot \mathbf{f}^{(t)}(\mathbf{x})\, \mathrm{d}S_x + \int_{V_{eK}} \mathbf{p} \cdot (\boldsymbol{e}_i\boldsymbol{e}_j + \boldsymbol{e}_j\boldsymbol{e}_i) \cdot \mathbf{s}^{(t)}(\mathbf{x})\, \mathrm{d}V_x \} \tag{24}$$

In eq 24, $\mathbf{p} = \mathbf{x} - \mathbf{d}$. These "elementary shape factor tensors", $\boldsymbol{\xi}^{(t)}$, must be determined in order to evaluate ξ, B, or $[\eta]$ for arbitrary rigid bead arrays. For an uncharged spherical particle with stick boundary conditions in one of the five elementary shear fields,

$$\xi^{(t)} = \frac{5}{2\gamma} \boldsymbol{E}^{(t)} \tag{25}$$

II.C. Single Bead Forces and Related Quantities. Consider a single bead, K, centered at $\mathbf{x}_K$ and translating through the solution with velocity $\mathbf{u}_K$. Also let $\mathbf{v}'_K$ denote what the fluid velocity would be at $\mathbf{x}_K$ if bead K were absent. The total force exerted by bead K on the fluid can be written

$$\mathbf{F}_K = \int_{S_K} \mathbf{f}(\mathbf{x})\, \mathrm{d}S_x + \int_{V_{eK}} \mathbf{s}(\mathbf{x})\, \mathrm{d}V_x = \zeta_{Kt}^{*}(\mathbf{u}_K - \mathbf{v}'_K) \tag{26}$$

In eq 26 ζ_{Kt}^{*} denotes the translational friction constant of bead K. In the absence of external forces, it is simply given by Stokes law, $6\pi\eta a_K$. It is also convenient to define

$$M_{Kji} = \int_{S_K} (x_i - x_{Ki}) f_j(\mathbf{x})\, \mathrm{d}S_x + \int_{V_{eK}} (x_i - x_{Ki}) s_j(\mathbf{x})\, \mathrm{d}V_x \tag{27}$$

$$N_{Kjim} = \int_{S_K} (x_i - x_{Ki})(x_m - x_{Km}) f_j(\mathbf{x})\, \mathrm{d}S_x + \int_{V_{eK}} (x_i - x_{Ki})(x_m - x_{Km}) s_j(\mathbf{x})\, \mathrm{d}V_x \tag{28}$$

Now the dyadic tensor, $\mathbf{M}_K$, is related to the torque and stress on bead K. Let $\mathbf{T}_K$ denote the torque exerted by bead K on the fluid about its origin, $\mathbf{x}_K$. The angular velocity of the bead array about $\mathbf{d}$ is $\boldsymbol{\omega}$, and this is also the angular velocity of bead K about $\mathbf{x}_K$. Also let $\mathbf{c}_K$ denote the corresponding angular velocity of the fluid about $\mathbf{x}_K$ if bead K were absent. Then

$$T_{Ki} = \sum_{j,k=1}^{3} \varepsilon_{ijk} M_{Kkj} = \zeta_{Kr}^{*}(\omega_i - c_{Ki}) \tag{29}$$

In eq 29, ε_{ijk} is the Levi-Civita symbol (which equals 1 for $(ijk) = (123), (231), (312)$; -1 for $(ijk) = (132), (321), (213)$; and 0 otherwise), and ζ_{Kr}^{*} is the rotational friction constant of bead K. In the absence of external forces, $\zeta_{\mathrm{Kr}}^{*} = 8\pi\eta a_{\mathrm{K}}^3$.

Now return to eq 24 and write

$$\mathbf{p} = (\mathbf{x} - \mathbf{x}_K) + \mathbf{r}_K \tag{30}$$

$$\mathbf{r}_K = \mathbf{x}_K - \mathbf{d} \tag{31}$$

Using eqs 26, 27, 30, and 31 in eq 24

$$\xi_{ij}^{(t)} = -\frac{1}{2\eta_0 \gamma V_{\mathrm{p}}} \sum_{K=1}^{N} \{ r_{Ki} F_{Kj}^{(t)} + r_{Kj} F_{Ki}^{(t)} + M_{Kji}^{(t)} + M_{Kij}^{(t)} \} \tag{32}$$

Equation 32 will be of considerable value in determining the elementary shape factor tensors of arbitrary rigid bodies. In the special case of a single bead, K, placed in elementary shear field, $\mathbf{E}^{(t)}$, eq 32 reduces to

$$\xi_K^{(t)} = \frac{\xi_K^{*}}{\gamma} \boldsymbol{E}^{(t)} = -\frac{1}{2\eta_0 \gamma V_K} (\boldsymbol{M}_K^{(t)} + \boldsymbol{M}_K^{(t)\mathrm{T}}) \tag{33}$$

The "T" superscript in eq 33 denotes transpose. ξ^*_K is the viscosity shape factor of a single isolated bead which equals $^5/_2$ in the limit of an uncharged sphere. In the present work, however, it shall be left as an adjustable parameter. It could, in fact, be negative which corresponds to a negative solute intrinsic viscosity which occurs in certain systems.[1,21] The local shear gradient in the vicinity of bead K is approximated with

$$E_{Kij} = v'_{Ki,j} + v'_{Kj,i} \tag{34}$$

$$v'_{Ki} = v'_i(\mathbf{x})\Big|_{\mathbf{x}_K} \tag{35}$$

$$v'_{Ki,j} = \frac{\partial v'_i(\mathbf{x})}{\partial x_j}\Big|_{\mathbf{x}_K} \tag{36}$$

In eqs 34−36, the fluid velocity is evaluated at the centroid of bead K, $\mathbf{x}_K$, with bead K removed. (In the course of this study, we also tried the more complicated procedure of averaging the fluid velocities over the surface of (removed) bead K, but actually obtained more accurate results with the simpler approach described above.) Equation 33 can be written

$$M_{Kij} + M_{Kji} = -2\eta_0 V_K \xi^*_K E_{Kij} \tag{37}$$

Equations 29 and 37 can be combined to yield

$$M_{Kij} = -\frac{\zeta^*_{Kr}}{2}\sum_{k=1}^{3}\varepsilon_{ijk}(\omega_k - c_{Kk}) - \eta_0 V_K \xi^*_K E_{Kij} \tag{38}$$

Equation 38 is useful since it gives the components of the tensor, $\mathbf{M}_K$, in terms of single bead solute transport parameters (ζ^*_{Kr} and ξ^*_K) and the relative velocity field of the fluid in the vicinity of bead K if bead K were absent ($\boldsymbol{\omega}$, $\mathbf{c}_K$, and $\mathbf{E}_K$). We can also write

$$c_{Ki} = -\frac{1}{2}\sum_{j,k=1}^{3}\varepsilon_{ijk}v'_{Kj,k} \tag{39}$$

The components of the triadic tensor, $\mathbf{N}_K$, defined by eq 28, are more difficult to deal with since they cannot, in general, be directly related to single bead transport parameters as is possible for $\mathbf{F}_K$ (eq 26) and $\mathbf{M}_K$ (eq 38). However, the special case of a single bead in the absence of external forces can be solved since the hydrodynamic forces, $\mathbf{f}(\mathbf{x})$, are well-known for a translating or rotating sphere, or for a sphere placed in a shear field. In this case, it can be shown

$$N_{Kjim} = \frac{a_K^{\,2}}{3}\delta_{im}F_{Kj} \tag{40}$$

Under these conditions, translation contributes, but not rotation or shear. In the present work, we shall approximate $N_{K\,jim}$ with eq 40. It should be noted that external forces do enter in general through F_{Kj}. As we show in the next section, the components of N_K enter as higher order correction terms in any case.

II.D. Calculation of F_K and $\mathbf{M}_K$. Following a boundary element procedure developed previously,[28] the fluid velocity at point $\mathbf{y}$ anywhere in space can be written[4]

$$\mathbf{v}(\mathbf{y})\Phi(\mathbf{y}, V_e) = \mathbf{v}_0(\mathbf{y}) - \sum_{K=1}^{N}\mathbf{v}_{\mathrm{RBM}}(\mathbf{y})\,\Phi(\mathbf{y}, V_K) + \sum_{K=1}^{N}\{\int_{S_K}\boldsymbol{U}(\mathbf{r})\cdot\mathbf{f}(\mathbf{x})\,\mathrm{d}S_x + \int_{V_{eK}}\boldsymbol{U}(\mathbf{r})\cdot\mathbf{s}(\mathbf{x})\,\mathrm{d}V_x\} \tag{41}$$

In eq 41, $\mathbf{v}_0(\mathbf{y})$ denotes the fluid velocity at $\mathbf{y}$ in the absence of all beads, $\mathbf{v}_{\mathrm{RBM}}(\mathbf{y})$ denotes the rigid body motion of the bead array (eq 1), V_K denotes the inner core volume of bead K, V_e is the fluid volume exterior to the inner core volumes, $\mathbf{f}(\mathbf{x})$ is the hydrodynamic force/area exerted by the bead on the fluid at $\mathbf{x}$, and $\Phi(\mathbf{y},V)$ equals 1 if $\mathbf{y}$ lies within V, it equals 0 if $\mathbf{y}$ lies outside of V, and it equals $^1/_2$ if $\mathbf{y}$ lies on the boundary surface enclosing V. Also, $\mathbf{r} = \mathbf{x} - \mathbf{y}$ and $\mathbf{U}(\mathbf{r})$ is the singular (Oseen) tensor defined by

$$\boldsymbol{U}(\mathbf{r}) = \frac{1}{8\pi\eta_0 r}\left(\boldsymbol{I} + \frac{1}{r^2}\boldsymbol{rr}\right) \tag{42}$$

Next, remove bead K and choose $\mathbf{y} = \mathbf{x}_K$ where $\mathbf{x}_K$ is the centroid of bead K. Also, expand $\mathbf{U}(\mathbf{r})$ in eq 41 to second order about $\mathbf{x}_{JK} = \mathbf{x}_J - \mathbf{x}_K$ and use the definitions of eqs 26−28

$$v'_{Ki} \cong v_{K0i} + \sum_{J\neq K}\left\{\sum_{j=1}^{3}U^{Ki}_{Jj}F_{Jj} + \sum_{j,k=1}^{3}U^{Ki}_{Jj,k}M_{Jjk} + \frac{1}{2}\sum_{j,k,m=1}^{3}U^{Ki}_{Jj,km}N_{Jjkm}\right\} \tag{43}$$

where v'_{K_i} is defined by eq 35, $v_{K0i} = (\mathbf{v}_0(\mathbf{x}_K))_i$,

$$U^{Ki}_{Jj} = U_{ij}(\mathbf{x}_{JK}) = \mathbf{e}_i\cdot\boldsymbol{U}(\mathbf{x}_{JK})\cdot\mathbf{e}_j \tag{44a}$$

$$U^{Ki}_{Jj,k} = \frac{\partial U_{ij}(\mathbf{r})}{\partial x_k}\Big|_{\mathbf{r}=\mathbf{x}_{JK}} \tag{44b}$$

$$U^{Ki}_{Jj,km} = \frac{\partial^2 U_{ij}(\mathbf{r})}{\partial x_k \partial x_m}\Big|_{\mathbf{r}=\mathbf{x}_{JK}} \tag{44c}$$

$$\nabla^2 U^{Ki}_{Jj} = \sum_{k=1}^{3}U^{Ki}_{Jj,kk} \tag{44d}$$

Truncating the expansion of U_{ij} at second order,(eq 44c), is accurate to order $x_{JK}{}^{-3}$. In what follows, we shall be careful to retain terms to this order.

Use eqs 26 and 40 in eq 43

$$F_{Ki} \cong \zeta^*_{Kt}(u_{Ki} - v_{K0i}) - \sum_{J\neq K}\left\{\sum_{j=1}^{3}\zeta^*_{Kt}\left(U^{Ki}_{Jj} + \frac{a_J^{\,2}}{6}\nabla^2 U^{Ki}_{Jj}\right)F_{Jj} + \sum_{j,k=1}^{3}\xi^*_{Kt}U^{Ki}_{Jj,k}M_{Jjk}\right\} \tag{45}$$

Using eqs 1 and 3 in eq 45,

$$\sum_{J=1}^{N}\sum_{j=1}^{3} Q_{Jj}^{Ki} F_{Jj} + \sum_{J=1}^{N}\sum_{j,k=1}^{3} B_{Jjk}^{Ki} M_{Jjk} + \sum_{j=1}^{3} L_{j}^{Ki}\delta\omega_j = a_{Ki} \tag{46}$$

where we have defined

$$Q_{Jj}^{Ki} = \delta_{KJ}\delta_{ij} + (1-\delta_{KJ})\zeta_{Kt}^{*}\left(U_{Jj}^{Ki} + \frac{a_J^{\,2}}{6}\nabla^2 U_{Jj}^{Ki}\right) \tag{47}$$

$$B_{Jjp}^{Ki} = \zeta_{Kt}^{*} U_{Jj,p}^{Ki} \tag{48}$$

$$L_{j}^{Ki} = -\zeta_{Kt}^{*}\sum_{k=1}^{3}\varepsilon_{ijk}(x_{Kk} - d_k) \tag{49}$$

$$\delta\omega_j = \omega_j - \omega_j^{\,0} \tag{50}$$

$$a_{Ki} = -\frac{\zeta_{Kt}^{*}}{2}\sum_{j=1}^{3} E_{oij}(x_{Kj} - d_j) \tag{51}$$

For the sake of convenience, all U_{Jj}^{Ki}, $U_{Jj,k}^{Ki}$, and $U_{Jj,km}^{Ki}$ terms with $J = K$ shall be included, but set to zero. This procedure shall simplify the notation in the remainder of this work. E_{0ij} in eq 51 is the shear field using $\mathbf{v}_0(\mathbf{x})$in eq 34. Equation 46 represents $3N$ equations in $12N + 3$ unknowns. The unknowns are the $3N$ components of $\{\mathbf{F}_J\}$ and the $9N$ components of $\{\mathbf{M}_J\}$, and the 3 components of $\boldsymbol{\delta\omega}$. Strictly speaking, the three components of the center of rotation, $\mathbf{d}$, are also unknown. However, for the applications of interest in this work, the center of mass and $\mathbf{d}$ coincide to a good approximation. For all of the applications in this work, $\mathbf{d}$ is approximated with the center of mass.

This is a good point to account for the effects of Brownian motion. This is a difficult problem that has been extensively addressed over many years and only some of this past work is cited here.[10,11,13,29,30] Perhaps the most authoritative treatment with regards to rigid structures is given by Brenner.[29] Relevant to the problem of significant Brownian motion, where $\gamma/D_r^* \ll 1$ (where D_r^* is the smallest eigenvalue of the rotational diffusion tensor of our bead array), and its effect on a suspension of dilute particles placed in a shear field, we need to include an additional angular velocity in the vicinity of each (removed) bead (see sections 7 and 8 of reference[29]). Quite simply and remarkably, this added term is equivalent to setting $\delta\omega_j = 0$ in eq 50. This is also the procedure used long ago by Simha.[10] In the remainder of this work, we shall follow this procedure and this reduces the number of unknowns to $12N$. A closely related problem involves the effect of structural flexibility. Zimm[30] pioneered the Monte Carlo procedure of approximating the transport of flexible structures with an equilibrium ensemble of rigid conformations. Later investigators showed how this approximation provided bounds on the intrinsic viscosity.[31,32] In the applications of duplex DNA and alkanes in benzene presented in this work, the Monte Carlo procedure of Zimm[30] shall be employed.

We also need the gradient of v'_{Ki} (eq 36). Following an analysis similar to that which led to eq 43,

$$v'_{Ki,m} \cong v_{K0i,m} - \sum_{J\neq K}\left\{\sum_{j=1}^{3} U_{Jj,m}^{Ki} F_{Jj} + \sum_{j,k=1}^{3} U_{Jj,km}^{Ki} M_{Jjk}\right\} \tag{52}$$

Using eq 52 in eqs 34 and 39, substituting these into eq 38, we obtain an additional $9N$ equations,

$$\sum_{J=1}^{N}\sum_{j=1}^{3} C_{Jj}^{Kim} F_{Jj} + \sum_{J=1}^{N}\sum_{j,p=1}^{3} H_{Jjp}^{Kim} M_{Jjp} = b_{Kim} \tag{53}$$

$$C_{Jj}^{Kim} = -\frac{\zeta_{Kr}^{*}}{4}(U_{Jj,m}^{Ki} - U_{Jj,i}^{Km}) - \eta_0 V_K \xi_K^{*}(U_{Jj,m}^{Ki} + U_{Jj,i}^{Km}) \tag{54}$$

$$H_{Jjp}^{Kim} = \delta_{KJ}\delta_{ij}\delta_{mp} - \frac{\zeta_{Kr}^{*}}{4}(U_{Jj,mp}^{Ki} - U_{Jj,ip}^{Km}) - \eta_0 V_K \xi_K^{*}(U_{Jj,mp}^{Ki} + U_{Jj,ip}^{Km}) \tag{55}$$

$$b_{Kim} = -\eta_0 V_K \xi_K^{*} E_{0im} \tag{56}$$

Equations 46 and 53 can be written in compact matrix form

$$\boldsymbol{Q}\cdot\mathbf{F} + \boldsymbol{B}\cdot\mathbf{M} = \mathbf{a} \tag{57}$$

$$\boldsymbol{C}\cdot\mathbf{F} + \boldsymbol{H}\cdot\mathbf{M} = \mathbf{b} \tag{58}$$

In eqs 57 and 58,$\underline{\mathbf{F}}$and $\mathbf{a}$are $3N$ by 1 column vectors formed by stacking $\mathbf{F}_1$, $\mathbf{F}_2$, ..., $\mathbf{F}_N$ and $\mathbf{a}_1$, $\mathbf{a}_2$, ..., $\mathbf{a}_N$ on top of each other. $\underline{\mathbf{M}}$ and $\underline{\mathbf{b}}$ are $9N$ by 1 column vectors formed by first writing the N dyadic (3 by 3) tensors, $\boldsymbol{M}_J$, and $\boldsymbol{b}_J$ as 9 by 1 column vectors. For example, we write for $\mathbf{M}'_J$:

$$\mathbf{M}'_J = \begin{pmatrix} M_{J11} \\ M_{J12} \\ M_{J13} \\ M_{J21} \\ \vdots \\ M_{J33} \end{pmatrix} \tag{59}$$

These N column vectors are stacked on top of each other to form $\mathbf{M}$. A similar procedure is used to construct $\mathbf{b}$. Also $\boldsymbol{Q}$, $\boldsymbol{B}$, $\mathbf{C}$, and $\mathbf{H}$ are $3N$ by $3N$, $3N$ by $9N$, $9N$ by $3N$, and $9N$ by $9N$ matrices, respectively. Consider, for example, the $\boldsymbol{B}$ matrix. B_{Jjp}^{Kj} is that element of $\mathbf{B}$ that occupies the $3*(K-1) + i$ row and $9*(J-1) + 3*(j-1) + p$ column. Similarly, H_{Jjp}^{Kjm} is that element of $\mathbf{H}$ that occupies the $9*(K-1) + 3*(i-1) + m$ row and $9*(J-1) + 3*(j-1) + p$ column. Note that the superscript indices on the $\boldsymbol{Q}$, $\boldsymbol{B}$, $\mathbf{C}$, and $\mathbf{H}$ matrices are row indices and the subscript indices are column indices.

Next, eqs 57 and 58 can be combined into a single "supermatrix" representation

$$\boldsymbol{G}\cdot\mathbf{F}^* = \mathbf{s}^* \tag{60}$$

$$\boldsymbol{G} = \begin{pmatrix} \boldsymbol{Q} & \boldsymbol{B} \\ \boldsymbol{C} & \boldsymbol{H} \end{pmatrix} \tag{61}$$

$$\mathbf{s}^* = \begin{pmatrix} \mathbf{a} \\ \mathbf{b} \end{pmatrix} \tag{62}$$

G is a 12*N* by 12*N* matrix; **F*** and **s*** are 12*N* by 1 column vectors. It should be emphasized that the submatrices $\boldsymbol{Q}$, $\boldsymbol{B}$, **C**, and **H** in eq 61 are not the same size. Specifically, $\boldsymbol{Q}$, $\boldsymbol{B}$, **C**, and **H** are 3*N* by 3*N*, 3*N* by 9*N*, 9*N* by 3*N*, and 9*N* by 9*N*, respectively. Once a structure is defined, all the components of **G** can be determined. Once an elementary shear field is defined, the components of **s*** can also be determined. Inversion of the $\boldsymbol{G}$ matrix yields $\mathbf{G}^{-1}$ and eq 60 can be written

$$\mathbf{F}^* = \boldsymbol{G}^{-1} \cdot \mathbf{S}^* \tag{63}$$

Once **F*** is obtained, eqs 23 and 32 can be used to compute ξ. From eq 19, this can then be used to determine B and $[\eta]$ for a single bead array averaged over all possible orientations in a simple shear field. The most time-consuming step in this procedure is the inversion of the 12*N* by 12*N* **G** matrix.

III. Results

III.A. Linear Strings and Rings of Beads. As discussed in previous work,[4,18] bead models made up of a small number of beads have historically not been very accurate unless account is taken of the variation of hydrodynamic stresses over the individual beads. The methodology employed in the present study is simpler than that used in reference4 in the sense that bead−bead interactions are only accounted for out to order a_J^2/r_{IJ}^3 (a_J is a bead radius and r_{IJ} is an interbead distance). Because of that, it is important to compare results using the methodology developed here with exact, or near exact results on certain systems.

In the present work, all model structures of interest shall consist of arrays of identical beads of radius a, and near neighbor separation, t. Define the three parameters; s_t, s_r, and s_v by the relations:

$$\zeta_t^* = s_t(6\pi\eta a) \tag{64a}$$

$$\zeta_r^* = s_r(8\pi\eta a^3) \tag{64b}$$

$$\xi^* = s_v(5/2) \tag{64c}$$

In the special case of no solute−solvent interactions beyond excluded volume interactions, s_t, s_r, and s_v can all be set to 1.00. This selection is made for the model studies in this subsection and in the next.

The model system relevant to the present work where exact results are available is the touching dimer ($t = 2a$) of two identical beads, where $\xi_{exact} = 3.45$.[33,34] (This value has recently been confirmed by detailed boundary element calculations. S. Aragon, personal correspondence, January, 2009). Recently, Garcia de la Torre and co-workers have carried out extrapolated shell calculations of bead oligomers. Each bead is modeled as a shell of many much smaller touching beads and the results extrapolated to the limit of an infinite number of smaller beads.[18] In Table 1, we summarize viscosity shape factors, ξ, for model results employing the procedure developed in the present work with these extrapolated shell values. The main purpose of reference[18] was not the shell model calculations themselves, but rather using them as benchmarks to test a simpler, more computationally efficient bead methodology valid in the absence of external forces. Those same shell model results are used here to test the present results. Agreement between the two lies within 5% of each other. It should be emphasized that results using the present methodology are not exact, but are nonetheless quite accurate for the special cases considered in Table 1. For additional tests/comparisons of other bead methodologies, the reader is referred to references 4, 14, and 18.

TABLE 1: Viscosity Shape Factors of Linear Strings and Rings of Touching Beads

structure[a]	ξ_{shell}[b]	ξ[c]
L2	3.42	3.43
L3	4.58	4.68
L4	5.98	6.22
R4	3.88	3.92
L5		7.56
L6	9.18	9.37
R6	4.80	4.90
L7		11.61
L8	13.10	13.19
L9		15.49
L10		18.78

[a] Linear, ring arrays of *N* beads denoted L*N*, R*N*, respectively. [b] From Shell Model results of reference 18. [c] From the present work.

III.B. Duplex DNA. In this subsection, the methodology shall be applied to the intrinsic viscosity of duplex DNA fragments of specific length. The viscosity experiments were carried out at 25 °C in a buffer solution of ionic strength 0.1 M (or higher) and extrapolated to zero shear.[35] Under these comparatively high salt conditions, electroviscous effects are expected to be small[25] and are ignored in the present work. Duplex DNA is modeled using the Hagerman discrete wormlike chain.[36,37] The hydrodynamic radius, R, of short duplex DNA modeled as a circular cylinder equals 1.0 ± 0.1 nm[38,39] and the contour length, L (in nm) equals $0.34n_{bp}$ where n_{bp} is the number of base pairs. To relate these parameters to a touching bead-discrete wormlike chain model of N beads of radius a, we set $L = 2Na$ and also set the volume of a right circular cylinder, $\pi R^2 L$, equal to that of N identical nonoverlapping beads, $4\pi Na^3/3$. This gives $a = (^3/_2)^{1/2}R = 1.225$ nm, $t = 2a = 2.45$ nm, and $n_{bp} = 7.2$ N. The persistence length, P, of DNA under the conditions of the experiment is expected to be approximately 50 nm.[40] Following Hagerman,[36,37] we randomly generate an "ensemble" (typically 100) of independent wormlike chains, compute the intrinsic viscosity and shape factor of each one treating it as a rigid body, and then average over all conformations to obtain an ensemble average. For the chains of interest in this work, an ensemble of 100 chains is sufficient to yield intrinsic viscosities that are accurate to within about 3%. The number of beads employed ranged from 16 (115 bp) to 86 (619 bp). This example illustrates the usefulness of the method in sampling a large number of conformations of a flexible chain. A randomly generated 86-bead wormlike chain with a persistence length of 40 nm, appropriate for 619 bp duplex DNA, is illustrated in Figure 2.

Shown in Figure 3 are experimental $[\eta]$'s along with model viscosities for rods (dashed line) and wormlike chains with $P = 50$ nm (dotted line) and 40 nm (solid line). The solvent viscosity, η_0, was set to 0.89 cP, appropriate for aqueous solutions at 25 °C. The parameters s_t, s_r, and s_v were all set to

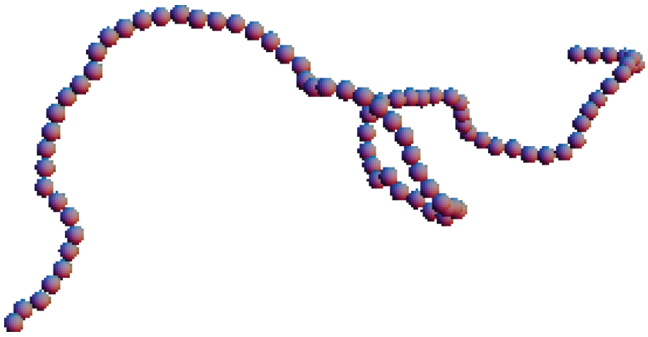

Figure 2. Representative wormlike chain for 619 base pair duplex DNA. The randomly generated chain consists of 86 beads with a persistence length of 40 nm (see the text for details).

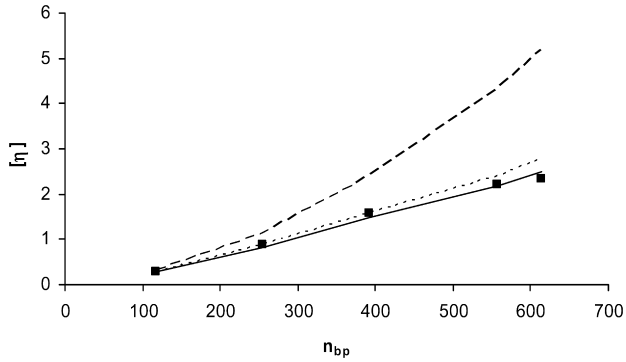

Figure 3. Intrinsic viscosity of DNA versus length. Experiments (filled squares) come from reference 35, were carried out at 25 °C in aqueous media, and intrinsic viscosities are in 10^2 cm^3/g. Model mobilities are rod (dashed line), $P = 50$ nm wormlike chain (dotted line), $P = 40$ nm wormlike chain (solid line). In the wormlike chain modeling studies, 100 conformations were averaged.

+1.0. A wormlike chain model with P in the 40 to 50 nm range is entirely consistent with experiment.

III.C. Alkanes in Benzene. A system which clearly deviates from the standard (S) model is alkanes in benzene where $[\eta]$ is negative when the molecular weight of the solute (alkane) is low.[1] Since the model developed in this work treats the solvent as a continuum, it should only be accurate on a distance scale comparable to or greater than the size of a solvent molecule, benzene in this case, or approximately 0.25 nm. However, the carbon−carbon bond length is 0.154 nm,[41] which means we have to choose our fundamental building block, or "monomer" to be larger than a single CH_2 group. On pragmatic grounds, we would like to choose our monomer to be small enough to capture the size dependence of $[\eta]$ observed experimentally, yet large compared to a solvent molecule or atom. In the analysis presented here, we choose our monomer unit as pentane, H−C_5H_{10}−H, which has a van der Waals excluded volume of 96.4 Å^3 = 0.0964 nm^3.[42] Setting this volume equal to that of a sphere of radius a, gives $a = 0.284$ nm. If we view C_5H_{12}, $C_{10}H_{22}$, $C_{15}H_{32}$, etc. as effectively one, two, three, etc. linear strings of touching beads, a logical choice for the interbead separation, t, is simply equal to $2a$ or 0.568 nm.

A quantity related to the flexibility of polymers of degree of polymerization n, in a good (theta) solvent is the dimensionless characteristic ratio, which can be defined

$$C_n = \frac{\langle r^2\rangle_0}{nh^2} \tag{65}$$

where $\langle r^2\rangle_0$ is the mean square end-to-end distance and h is the carbon−carbon bond length (0.154 nm). For polymethylene

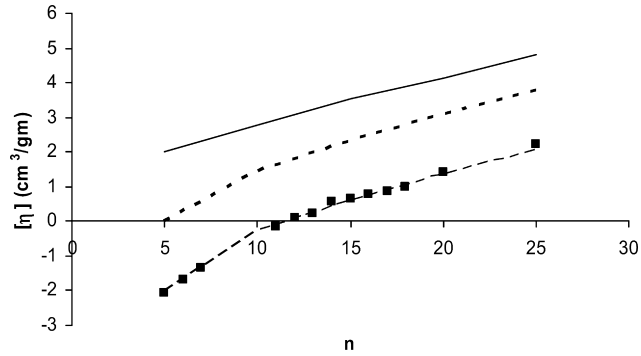

Figure 4. Intrinsic viscosity of alkanes in benzene versus length. Experiments (filled squares) come from reference 1 and were carried out at 25 °C. Solid, dotted, and dashed curves come from model studies with $s_v = +1.0$, 0.0, and −1.0, respectively.

under theta solvent conditions, $C_n = 6.6-6.8$ for large n.[43] For a long wormlike chain of persistence length P made up of $N = n/5$ structural units of bead spacing t, $\langle r^2\rangle_0 = 2PNt = 0.4nPt$,[43] eq 65 can be rearranged to give

$$P = \frac{C_n h^2}{2t}\left(\frac{n}{N}\right) \cong 0.68 \text{ nm} \tag{66}$$

Since benzene at room temperature does not constitute a theta solvent for low molecular weight alkanes, the actual persistence length may be different from 0.68 nm. Nonetheless, this value along with our choices for a and t, provide reasonable model parameters for the system of interest. Also, set $T = 25$ °C and $\eta_0 = 0.652$ cP (for benzene at 25 °C).

An estimate for s_v can now be made from the experimental value of $[\eta]$ for pentane in benzene.[1] From eqs 19 and 64c,

$$s_v = \frac{2M[\eta]}{5N_{Av}V_P} \tag{67}$$

In eq 67, M, $[\eta]$, and V_P all refer to the monomer unit, which in this case is pentane. With $M = 72$ g/mol, $[\eta] = -2.07$ cm^3/g,[1] and $V_P = 96.4$ Å^3,[42] $s_v \cong -1.00$. Since we do not have values for s_t and s_r, these are both set to +1.00. If, for example, experimental values were available for the translational and rotational diffusion constants of pentane in benzene, s_t and s_r could be defined more precisely.

Summarized in Figure 4 are experimental (filled squares from reference 1) and model intrinsic viscosities of alkanes in benzene. The solid, dotted, and dashed lines come from model studies with $s_v = +1.0$, 0.0, and −1.0, respectively. The other parameters for the model studies have been defined previously. For $N = 3-5$ (corresponding to $C_{15}H_{32}$ to $C_{25}H_{52}$), we followed a procedure similar to that described in section IIIB. Intrinsic viscosities were calculated for 100 independent wormlike chains and the results were averaged. As can be seen from Figure 4, the model studies with $s_v = -1.0$ reproduce very well the experimental $[\eta]$'s.

IV. Summary

The principle objectives of this work have been to generalize the S model for bead arrays, test this model's accuracy, and then apply it to two very different systems: duplex DNA in aqueous media and alkanes in benzene. The model development was presented in section II and the testing and applications in

section III. Within the framework of the S model, viscosity shape factors for dimers and linear strings and rings of touching beads are accurately reproduced with the methodology developed here. The S model is also able to explain very well the intrinsic viscosity of duplex DNA (in aqueous media) in the size range of 100 to over 600 base pairs when modeled as wormlike chains with a persistence length of between 40 and 50 nm.

Past studies of solute−solvent interactions as they relate to intrinsic viscosity have been handled differently by different investigators. A longstanding approach has been to simply add a constant term to the standard (S model) intrinsic viscosity to account for solute−solvent interactions.[1,44,45] Although this approach appears to work well, it is difficult to explain why it works in the context of the coarse grained methodology developed in the present work. In other words, we cannot explain how the short-range solute−solvent interactions appear to "uncouple" from the long-range hydrodynamic interactions. Lodge and co-workers[2,46,47] have advanced a model in which it is argued that solute can alter the "microviscosity"[47] of the solvent. Evidence in support of this comes from measurements of solvent rotation times and how these rotation times are altered by solute. However, this interpretation has been criticized.[48] Fixman also raised specific criticisms of the concept of a "microviscosity" that varies on a molecular distance scale.[21] The present work has been strongly influenced by that of Fixman[21] and draws on many of the ideas advanced in this earlier work.

The example of alkanes in benzene serves to illustrate both the strengths and shortcomings of the methodology developed in this work. On the positive side, we are able to account quite well for the length dependence of $[\eta]$ observed experimentally for reasonable choices of model input parameters. It is also able to sample many conformations of a flexible structure rapidly and efficiently. On the other hand, modeling the solvent as a continuum limits one to distance scales comparable to or larger than the size of the solvent molecules themselves. Finally, we are not, at the present time, able to give a microscopic interpretation for s_v. It was chosen to reproduce the experimental $[\eta]$ for pentane (our monomer) in benzene. These shortcomings aside, it is our hope that the methodology developed here will be useful to other investigators in viscosity studies of relatively low molecular weight solutes.

References and Notes

(1) Dewan, K. K.; Bloomfield, V. A.; Berget, P. G. *J. Phys. Chem.* **1974**, *75*, 3120.
(2) Meerwall, E. D.; Amelar, S.; Smeltzly, M. A.; Lodge, T. P. *Macromolecules* **1989**, *22*, 295.
(3) Banipal, T. S.; Singh, G. *Thermochim. Acta* **2004**, *412*, 63.
(4) Allison, S. A.; Pei, H. *J. Phys. Chem. B* **2009**, *113*, 8056.
(5) Happel, J., Brenner, H., *Low Reynolds Number Hydrodynamics*; Martinus Nijhoff: The Hague, 1983.
(6) Kim, S., Karilla, S. J., *Microhydrodynamics*; Butterworth-Heinemann: Boston, MA, 1991.
(7) Hu, C.-M.; Zwanzig, R. *J. Chem. Phys.* **1974**, *60*, 4354.
(8) Einstein, A. *Ann. Phys.* **1911**, *34*, 591.
(9) Jeffrey, G. B. *Proc. R. Soc. London* **1923**, *A102*, 161.
(10) Simha, R. *J. Phys. Chem.* **1940**, *44*, 25.
(11) Scheraga, H. A. *J. Chem. Phys.* **1955**, *23*, 1526.
(12) Kirkwood, J. G.; Riseman, J. *J. Chem. Phys.* **1948**, *16*, 565.
(13) Kirkwood, J. G. , *Macromolecules*; Auer, E. P., Ed.; Gordon and Breach: New York, 1967.
(14) Garcia de la Torre, J.; Bloomfield, V. A. *Biopolymers* **1978**, *17*, 1605.
(15) Garcia Bernal, J. M.; Garcia de la Torre, J. *Biopolymers* **1980**, *19*, 751.
(16) Byron, O. *Biophys. J.* **1997**, *72*, 408.
(17) Garcia de la Torre, J. *Biophys. Chem.* **2001**, *93*, 159.
(18) Garcia de la Torre, J.; del Rio Echenique, G.; Ortega, A. *J. Phys. Chem. B* **2007**, *11*, 955.
(19) Allison, S. A. *Macromolecules* **1999**, *32*, 5304.
(20) Hahn, D. K.; Aragon, S. *J. Chem. Theory Comput.* **2006**, *2*, 1416.
(21) Fixman, M. *J. Chem. Phys.* **1990**, *92*, 6858.
(22) Bauer, D. R.; Brauman, J. I.; Pecora, R. *J. Am. Chem. Soc.* **1974**, *96*, 6840.
(23) Booth, F. *Proc. R. Soc., London* **1950**, *A203*, 533.
(24) Sherwood, J. D. *J. Fluid Mech.* **1980**, *101*, 609.
(25) Allison, S. A. *Macromolecules* **1998**, *31*, 4464.
(26) Batchelor, G. K. *J. Fluid Mech.* **1970**, *41*, 545.
(27) Russel, W. B. *J. Colloid Interface Sci.* **1976**, *55*, 590.
(28) Allison, S. A.; Nambi, P. *Macromolecules* **1992**, *25*, 3971.
(29) Brenner, H. *Chem. Eng. Sci.* **1972**, *27*, 1069.
(30) Zimm, B. H. *Macromolecules* **1980**, *13*, 592.
(31) Wilemski, G.; Tanaka, G. *Macromolecules* **1981**, *14*, 1531.
(32) Fixman, M. *J. Chem. Phys.* **1983**, *78*, 1588.
(33) Wakiya, S. *J. Phys. Soc. Jpn.* **1971**, *31*, 1581. Wakiya, S. *J. Phys. Soc. Jpn.* **1972**, *33*, 278.
(34) Brenner, H. *Int. J. Multiphase Flow* **1974**, *1*, 195.
(35) Tanigawa, M.; Mukaiyama, N.; Shimokubo, S.; Wakabayashi, K.; Fujita, Y.; Fukudome, K.; Yamaoka, K. *Polymer J. (Tokyo)* **1994**, *26*, 291.
(36) Hagerman, P. J.; Zimm, B. H. *Biopolymers* **1981**, *20*, 1481.
(37) Hagerman, P. J. *Biopolymers* **1981**, *20*, 1503.
(38) Eimer, W.; Williamson, J. R.; Boxer, S. G.; Pecora, R. *Biochemistry* **1990**, *29*, 799.
(39) Diaz, R.; Fujimoto, B. S.; Schurr, J. M. *Biophys. J.* **1997**, *72*, A322.
(40) Schellman, J. A.; Harvey, S. C. *Biophys. J.* **1995**, *55*, 95.
(41) McMurry, J., *Organic Chemistry*, 7th ed.; Thomson, Brooks, and Cole: Australia, 2008; Chapter 1.
(42) Edward, J. T. *J. Chem. Educ.* **1970**, *47*, 261.
(43) Flory, P. J., *Statistical Mechanics of Chain Molecules*; Interscience Publishers: New York, 1969.
(44) Garcia de la Torre, J.; Freire, J. J. *Macromolecules* **1982**, *15*, 155.
(45) Abe, F.; Einaga, Y.; Yamakawa, H. *Macromolecules* **1991**, *24*, 4423.
(46) Lodge, T. P. *J. Phys. Chem.* **1993**, *97*, 1480.
(47) Lodge, T. P.; Krahn, J. R. *Macromolecules* **1994**, *27*, 6223.
(48) Yoshizaki, T.; Takaeda, Y.; Yamakawa, H. *Macromolecules* **1993**, *26*, 6891.

JP907020J